Y^*K and Y^*K^* production in π^+p interactions at 10.3 GeV/c

M. C. Goddard, A. W. Key, G. J. Luste, J. D. Prentice, and T.-S. Yoon
Department of Physics, University of Toronto, Toronto, Ontario M5S 1A7, Canada

H. A. Gordon and K. W. Lai
Brookhaven National Laboratory, Upton, Long Island, New York
(Received 2 August 1978)

The reactions $\pi^+p \to \Sigma^+(1385)K^+$ and $\pi^+p \to \Sigma^+(1385)K^{*+}(890)$ are examined. The $\Sigma^+(1385)K^+$ differential cross section for $-t' < 0.5$ GeV^2 and spin density matrix elements agree with a Regge-pole model incorporating (nondegenerate) vector and tensor K^* exchange with dominant $M1$ coupling. The $\Sigma^+(1385)K^{*+}(890)$ density matrix elements are consistent with the quark-additivity predictions. A Y^{*+} at a mass of 1700 MeV is also observed in the $\Lambda\pi^+$ mass distribution, produced opposite both K^+ and $K^{*+}(890)$.

INTRODUCTION

In this paper we study $Y^{*+}K^+$ and $Y^{*+}K^{*+}(890)$ quasi-two-body production in the $\Lambda K\pi$ and $\Lambda K2\pi$ final states produced in π^+p interactions at 10.3 GeV/c. For the purposes of this work Y^{*+} denotes both the $\Sigma^+(1385)$ and a higher-mass state which we observe as an enhancement in the $\Lambda\pi^+$ mass distribution from both the $\Lambda K\pi$ and $\Lambda K2\pi$ final states. This structure has a mass of approximately 1700 MeV, and we refer to it as $\Sigma^+(1700)$.

We examine the production of $\Sigma^+(1385)$ and $\Sigma^+(1700)$ opposite both K^+ and $K^{*+}(890)$ using the differential cross sections and the $\Sigma^+(1385)$, $K^{*+}(890)$ spin density matrix elements. For $\Sigma^+(1385)K^+$ production we compare our data with the predictions of a specific Regge-pole model. We examine the quark-additivity predictions for

$$\Sigma^+(1385)K^{*+}(890)$$

production. We attempt to determine the $\Sigma^+(1700)$ spin by examining the decay-angular moments from both

$$\Sigma^+(1700)K^+$$

and

$$\Sigma^+(1700)K^{*+}(890)$$

final states.

THE EXPERIMENT

The results presented here come from a 580 000-picture exposure of the SLAC 82-in. bubble chamber using an rf-separated π^+ beam of momentum 10.3 GeV/c. The incident-beam flux was approximately 10 tracks/picture, giving an experimental sensitivity of 31.1 ± 0.2 events/μb (see Ref. 1 for further experimental details).

The film was scanned for events with at least one visible strange-particle decay. Each event was then kinematically reconstructed from the images on film and fitted to various strange-particle final-state hypotheses. For every fit the predicted film bubble density for each track was required to be consistent with that observed on the film. When this procedure resulted in more than one fit for an event, only that fit (or fits) with the highest number of constraints was (were) kept. Fits having a χ^2 probability of less than 2% were deleted. Events having more than one fit after this selection procedure were flagged as ambiguous. In addition, a small number of events were deleted based on strange-particle decay lengths and opening angles. Further details may be found in Ref. 1.

The ambiguous events were assigned that fit having the lowest χ^2 value. The number of unique and ambiguous fits together with the cross sections, for the final states discussed in this paper, are listed in Table I (from Ref. 1.).

As the table indicates, a large number of the $\Lambda K2\pi$ events are ambiguous. By choosing the fit with the lowest χ^2 value the possibility of assigning some of these fits incorrectly is always present. However, since in this paper we are interested only in events lying within relatively narrow mass bands, this contamination should be minimal. We have found no significant differences in our results when only unique events are used.

For the $\Lambda K^+\pi^+$ channel the visible Λ decay and the absence of other neutral particles leads to a highly constrained kinematic fit with minimal contamination from other final states. As the table indicates, the number of ambiguous fits is very small.

TABLE I. Cross sections and numbers of events for $\Lambda K\pi$, $\Lambda K2\pi$ final states.

Final state	Number of events	Number of unique events	Channel cross section (from Ref. 1) (μb)
$\Lambda K^+\pi^+$	344	321	30 ± 2
$\Lambda K^+\pi^+\pi^0$	939	481	87 ± 3
$\Lambda K^0\pi^+\pi^+$	727	307	43 ± 6

$Y^{*+}K^+$ PRODUCTION IN THE $\Lambda K^+\pi^+$ FINAL STATE

The production of the $\Lambda K^+\pi^+$ final state at this energy is dominated by two quite different dynamical mechanisms. Figure 1 shows the $\Lambda K^+\pi^+$ Dalitz plot which indicates two distinct regions (see also Fig. 1 of Ref. 2). The region showing a threshold ΛK^+ enhancement has been investigated elsewhere,[2] where we concluded that it was due to proton diffraction dissociation. The other region corresponds to $Y^{*+}K^+$ production, and is the subject of this section.

In Fig. 2 we show the $\Lambda\pi^+$ mass distribution fitted to two Breit-Wigner functions multiplied by phase space, plus a phase-space background. We obtain fitted mass and width values of

$$M_1 = 1389\pm6 \text{ MeV}, \quad \Gamma_1 = 35\pm9 \text{ MeV},$$

$$M_2 = 1698\pm20 \text{ MeV}, \quad \Gamma_2 = 240\pm60 \text{ MeV}.$$

The bump at approximately 1700 MeV is a common feature of the $\Lambda\pi$ mass spectrum observed in production experiments [referred to as $\Sigma(1690)$ in Ref. 3]. The mass appears to be too high and the width too broad to be associated solely with the $\Sigma(1670)$, which is seen primarily in the $\Sigma\pi$ and $\Sigma\pi\pi$ decay modes.[4] It may be composed of more than one state, as appears to be the case for the $\Sigma(1670)$, although we see no obvious evidence for this in the mass distribution. Our statistics are too limited to investigate this question in more detail, and we will simply refer to this bump as $\Sigma(1700)$ and treat it as a single resonant state.

Figure 3 shows the Chew-Low plot for $\Lambda K^+\pi^+$. The $\Sigma^+(1385)$ and $\Sigma^+(1700)$ are seen to be produced almost entirely with $-t<1.0$ GeV^2.

We find the cross section for

$$\pi^+p \to \Sigma^+(1700)K^+ \quad (1)$$
$$\searrow \Lambda\pi^+$$

to be 6 ± 2 μb. This is shown in Fig. 4, together with results from two lower-energy experiments. We see no evidence for $\Sigma^+(1700)$ production in the final states $p\bar{K}^0K^+$, $(\Sigma\pi)^+K^+$. We obtain the following 95% confidence-level upper limits:

$$\pi^+p \to \Sigma^+(1700)K^+ < 1.5 \ \mu\text{b},$$
$$\searrow p\bar{K}^0$$

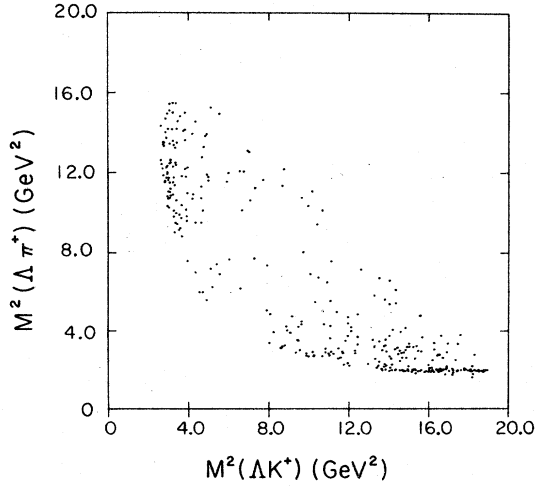

FIG. 1. Dalitz plot for the $\Lambda K^+\pi^+$ final state.

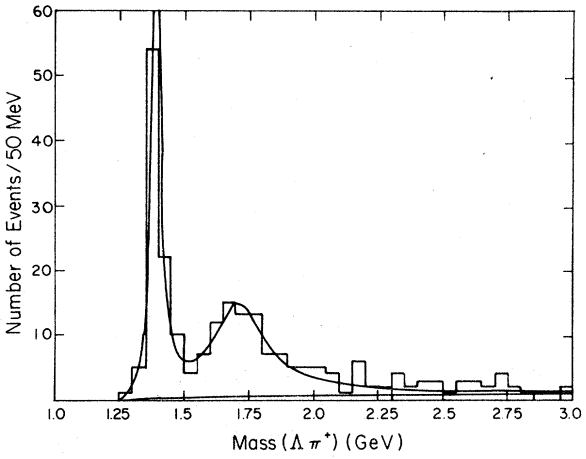

FIG. 2. $\Lambda\pi^+$ invariant-mass distribution from the $\Lambda K^+\pi^+$ final state.

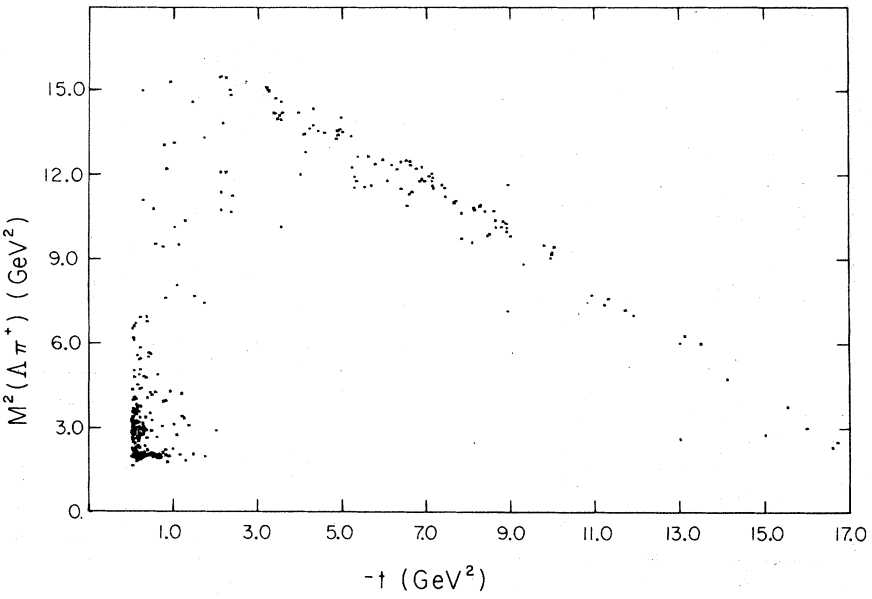

FIG. 3. Chew-Low plot for the $\Lambda K^+\pi^+$ final state.

$$\pi^+ p \to \Sigma^+(1700) K^+ < 4\ \mu\text{b}, \quad \Sigma^+(1700) \to (\Sigma\pi)^+$$

consistent with a dominant $\Lambda\pi$ decay of $\Sigma(1700)$.

Figure 5 shows $d\sigma/dt'$ for the $\Sigma^+(1700)$ region $[1.6 < M(\Lambda\pi^+) < 1.8$ GeV$]$.[5] The distribution gives a good fit to the functional form $A\exp(bt')$ with $b = 6.8 \pm 2.0$ GeV^{-2}.

In Fig. 6 we show the distribution of $\cos\theta$, where θ is the angle in the $\Lambda\pi^+$ rest frame between the direction of the Λ and the normal to the $Y^{*+}K^+$ production plane, the transversity frame. We have folded $\cos\theta$ around 0. The accumulation of events near $\cos\theta = \pm 1$ in the $\Sigma^+(1385)$ region is evident, in contrast to the isotropic distribution in the $\Sigma^+(1700)$ region. Figure 7(b) shows the (unfolded) projection of this distribution for $1.6 < M(\Lambda\pi^+) < 1.8$ GeV. The decay-angular distribution gives a satisfactory fit to isotropy with no improvement in the confidence level when a $\cos^2\theta$ term is added. We have also computed the moments up to $L = 5$ from the decay-angular distribution and the distribution of the longitudinal polarization of the Λ in the transversity frame; all are consistent with zero. This indicates that a spin-$\frac{1}{2}$ assignment is sufficient, although higher spins cannot

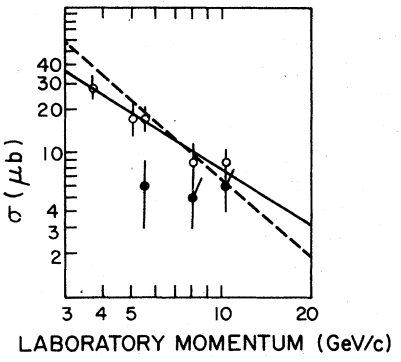

FIG. 4. $Y^{*+}K^+$ production cross section vs beam momentum. Open symbols refer to $\Sigma^+(1385)$ and closed symbols to $\Sigma^+(1700)$. The solid curve is the result of a fit to the $\Sigma^+(1385)$ data using $\sigma \propto P_{\text{lab}}^{-n}$. The dashed curve is the prediction of a Regge-pole model for $\Sigma(1385)$ production. Data points at other than 10.3 GeV/c are obtained from Refs. 6–9.

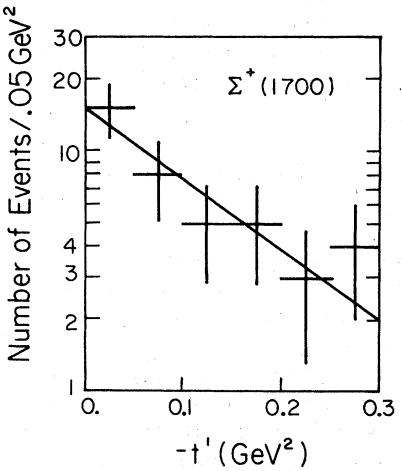

FIG. 5. $d\sigma/dt'$ for $\Sigma^+(1700)K^+$ (arbitrary units). The curve is the result of a fit using $d\sigma/dt' \propto e^{bt'}$, resulting in $b = 6.8 \pm 2.0$ GeV^{-2}.

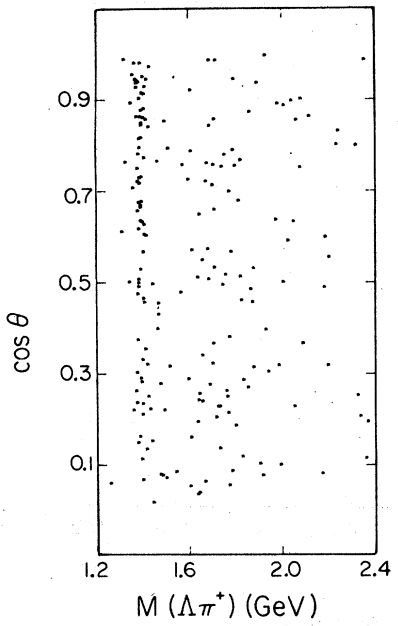

FIG. 6. Polar angle of the Λ from $\Lambda K^+\pi^+$ in the $\Lambda\pi^+$ rest frame relative to the $Y^{*+}K^+$ production normal vs mass of the $\Lambda\pi^+$ system.

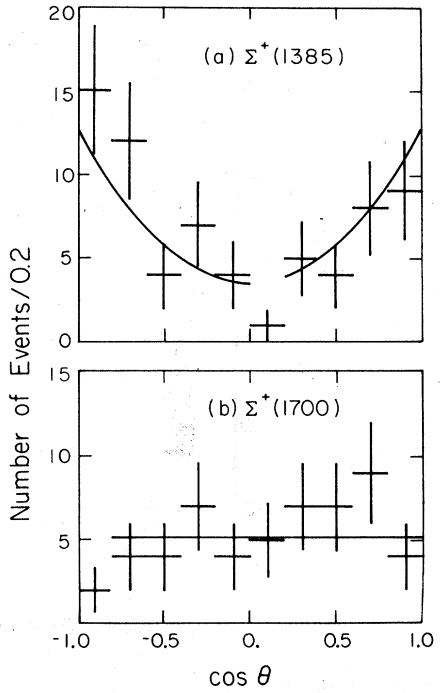

FIG. 7. Decay-angular distribution of Y^{*+} from $Y^{*+}K^+$ relative to the production normal. (a) $\Sigma^+(1385)$ region. The curve represents a fit to $1+A\cos^2\theta$; (b) $\Sigma^+(1700)$ region with a line representing an isotropic distribution.

be excluded.

Correcting for unseen decay modes,[3] we obtain a cross section for

$$\pi^+p \to \Sigma^+(1385)K^+ \qquad (2)$$

of 9 ± 2 μb. Figure 4 shows the reaction (2) cross section as a function of beam momentum ($P_{\rm lab}$). We use only experiments which are sensitive to the entire t' range (i.e., bubble-chamber experiments) and exclude threshold effects by selecting experiments with $P_{\rm lab}>3$ GeV/c. This results in the inclusion of results on reaction (2) contained in Refs. 6–9, but not those of Refs. 10–16. Parametrizing the cross section as

$$\sigma = AP_{\rm lab}^{-n},$$

we obtain $n=1.3\pm0.4$, slightly lower, but consistent with Aderholz *et al.*,[6] who found $n=1.7\pm0.4$.

In contrast to the $\Sigma^+(1700)$ region, Figs. 6 and 7(a) indicate structure in the decay-angular distribution of the $\Sigma^+(1385)$. A fit to $(1+A\cos^2\theta)$ yields $A=2.6\pm0.8$.

Figure 8 shows $d\sigma/dt'$ for $1.35<M(\Lambda\pi^+)<1.42$ GeV, normalized to the reaction (2) cross section. Here the differential cross section shows a flattening off for $-t'\simeq0.1$ GeV^2 and then a dip in the extreme forward direction. This is characteristic of a dominant helicity flip amplitude and is present in this reaction at lower energies[7-9] and in the line-reversed reaction.[17-19]

Using the method of moments we have computed the independent spin density matrix elements for the $\Sigma^+(1385)$ region. The real parts of the elements are shown in Fig. 9 as a function of t' in both the Gottfried-Jackson (t-channel) and the helicity (s-channel) coordinate systems. We see that the values are qualitatively similar in both reference systems, even away from the forward direction. Using the (weak) decay of the Λ from the $\Sigma^+(1385)$ (strong) decay, we have also computed the independent imaginary parts of the spin density matrix elements.[20] These are listed in Table II, together with the real parts, for $-t'<1.0$ GeV^2. The imaginary parts have large errors, and are consistent with zero; however, they are constrained to be close to zero from the positivity conditions.[21] Figure 10 shows the variation with laboratory momentum of the real parts of the spin density matrix elements averaged over $-t'$ in the Gottfried-Jackson coordinate system.

Assuming only $K^*(890)$ exchange, the Stodolsky-Sakurai assumption of $M1$ coupling at the K^*NY^* vertex predicts a $(1+3\cos^2\theta)$ decay-angular distribution of the $\Sigma^+(1385)$ relative to the production normal.[22,23] This implies[24]

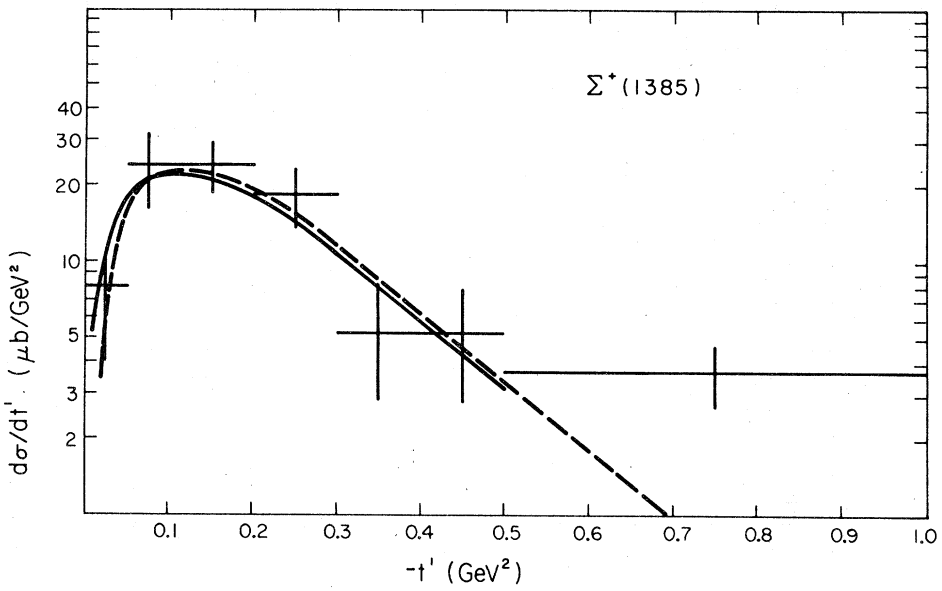

FIG. 8. $d\sigma/dt'$ for $\Sigma^+(1385)K^+$ (normalized to the total cross section, Ref. 26). The solid curve is the Stodolsky-Sakurai prediction with form factor, and the dashed curve is a Regge-pole-model prediction.

$$\rho_{33}=0.375, \quad \mathrm{Re}\,\rho_{3-1}=0.216, \quad \mathrm{Re}\,\rho_{31}=0$$

in both the Gottfried-Jackson and helicity coordinate systems.[25] These values are indicated in Figs. 9 and 10. They are consistent with our results for $0<-t'<1.0$ GeV^2 (Fig. 9), and are also consistent with the lower-energy data (Fig. 10). There is, perhaps, some indication that the agreement of ρ_{33} with the Stodolsky-Sakurai value becomes better with increasing energy.

The Stodolsky-Sakurai prediction for the differential cross section[22,23] gives reasonable agreement with the data at energies near threshold,[13,14,16] but at higher energies inclusion of an arbitrary form factor (e^{bt}) is necessary to obtain a good fit to the data. Including this form factor gives the result (normalized to our cross section) shown by the solid curve in Fig. 8.[26] The agreement is good for $-t'<0.5$ GeV^2, the dip in the forward direction being well reproduced. The defect in this, and in all non-Regge particle-exchange models, is the inability to reproduce the rapidly falling cross section as a function of beam momentum. In the present case the introduction of absorption fails to remedy this situation.[27-29]

A Regge-pole model using both vector and tensor K^* trajectories and incorporating $M1$ dominance and SU(3) symmetry has been advocated by Renninger and Sarma.[30,31] Our calculation using this model leads to the (absolute) prediction shown by the dashed curve in Fig. 8. The agreement with the data is good except for $-t'>0.5$ GeV^2. The predicted values of the density matrix elements are the same as the Stodolsky-Sakurai values, and we have seen that these agree with the data. In addition we now obtain the theoretical prediction for the energy dependence of the cross section, shown in Fig. 4 ($\sigma \propto P_{\mathrm{lab}}^{-n}$, $n=1.79$). The trend of the data is reproduced, and the value of n is consistent, with errors, both with our result and with that of Aderholz *et al.*[6]

The Stodolsky-Sakurai values for the spin density matrix elements also follow directly from the assumption of quark additivity[32] in the scattering process.[33] They are an example of the class A relations which follow directly from the additivity assumption.[34] They are found to give good agreement with a variety of different reactions at different energies.[35] However, a large statistics study of the line reversal of reaction (2)

TABLE II. $\Sigma^+(1385)$ Spin density matrix elements for $-t'<1.0$ GeV^2 from the $\Sigma^+(1385)K^+$ final state.

	Gottfried–Jackson frame	Helicity frame
ρ_{33}	0.38 ± 0.07	0.30 ± 0.07
$\mathrm{Re}\,\rho_{3-1}$	0.18 ± 0.07	0.23 ± 0.06
$\mathrm{Im}\,\rho_{3-1}$	0.11 ± 0.17	-0.03 ± 0.18
$\mathrm{Re}\,\rho_{31}$	-0.01 ± 0.05	0.04 ± 0.06
$\mathrm{Im}\,\rho_{31}$	0.26 ± 0.34	0.18 ± 0.33
$\mathrm{Im}\,\rho_{3-3}$	-0.36 ± 0.26	-0.22 ± 0.22
$\mathrm{Im}\,\rho_{1-1}$	0.23 ± 0.37	0.38 ± 0.40

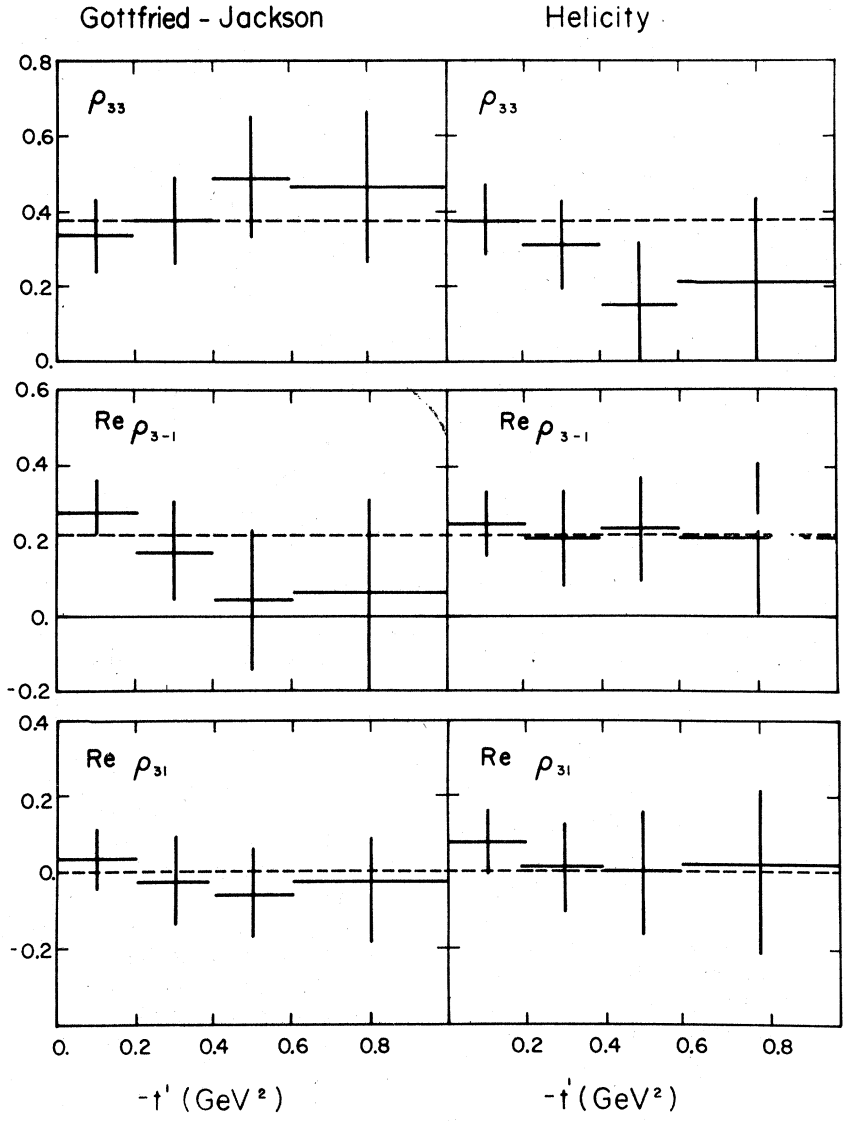

FIG. 9. $\Sigma^+(1385)$ spin density matrix elements [from $\Sigma^+(1385)K^+$] as a function of t' in the Gottfried-Jackson and helicity reference frames. The Stodolksy-Sakurai (quark-additivity) values are indicated by dashed lines.

has shown some violations near the forward direction.[19] Our errors are too large to allow observation of these violations in our data on reaction (2).

$Y^{*+}K^{*+}(890)$ PRODUCTION IN THE $\Lambda K2\pi$ FINAL STATES

Figure 11(a) shows the $(K\pi)^+$ mass distribution from the combined $\Lambda K^+\pi^+\pi^0$ and $\Lambda K^0\pi^+\pi^+$ (2 combinations/event) final states. In Fig. 11(b) we see that the background is considerably reduced when we choose the recoil mass to be in the $\Sigma^+(1385)$ region. Similarly, Fig. 12(a) shows the $\Lambda\pi^+$ mass distribution from the $\Lambda K2\pi$ final states. The $\Sigma^+(1385)$ is apparent, and there is a large accumulation of events in the low-mass region. Figure 12(b) shows the effect of selecting the recoil mass to be in the $K^{*+}(890)$ region. The background under the $\Sigma^+(1385)$ is reduced and a bump in the $\Sigma^+(1700)$ region has appeared. Fitting this mass distribution to two Breit-Wigner functions multiplied by phase space plus a phase-space background, we obtain mass and width values of

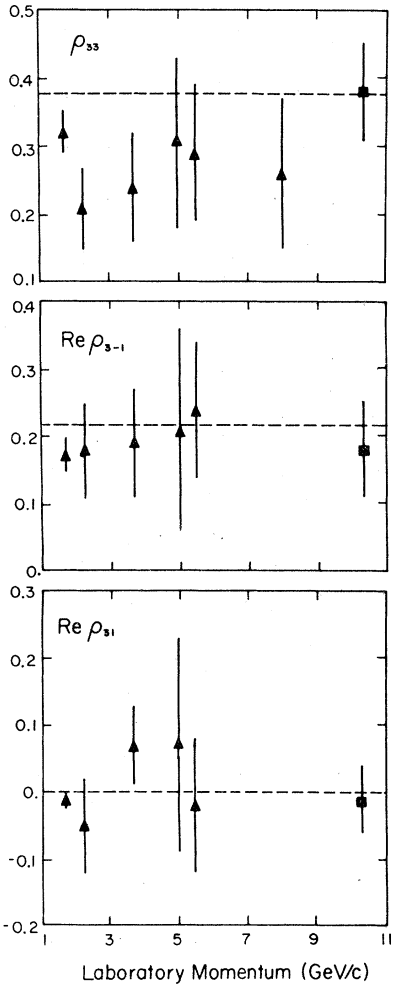

FIG. 10. $\Sigma^+(1385)$ spin density matrix elements from $\Sigma^+(1385)K^+$ in the Gottfried-Jackson frame as a function of beam momentum. The Stodolsky-Sakurai (quark-additivity) predictions are indicated by dashed lines. Our value is indicated by a square, the other values are obtained from Refs. 6–9, 13, 14.

$$M_1 = 1387 \pm 5 \text{ MeV}, \quad \Gamma_1 = 37 \pm 9 \text{ MeV},$$

$$M_2 = 1707 \pm 20 \text{ MeV}, \quad \Gamma_2 = 130 \pm {}^{100}_{60} \text{ MeV}.$$

We conclude that the $\Sigma^+(1700)$ is also present in the $\Lambda K 2\pi$ final states.

Figure 13 shows the Chew-Low plot for $\Lambda\pi^+K^{*+}(890)$. It is similar to that for the $\Lambda K^+\pi^+$ final state with dominantly peripheral production of $\Sigma^+(1385)$, $\Sigma^+(1700)$.

Figure 14 shows the differential cross section for $\Sigma^+(1700)K^{*+}(890)$ production ($0.85 < M(K\pi)^+ < 0.95$ GeV, $1.6 < M(\Lambda\pi^+) < 1.8$ GeV). From a fit to the form $A \exp(bt')$, we obtain $b = 3.2 \pm 1.3$ GeV^{-2}. The background in this case is large (we estimate about 50%).

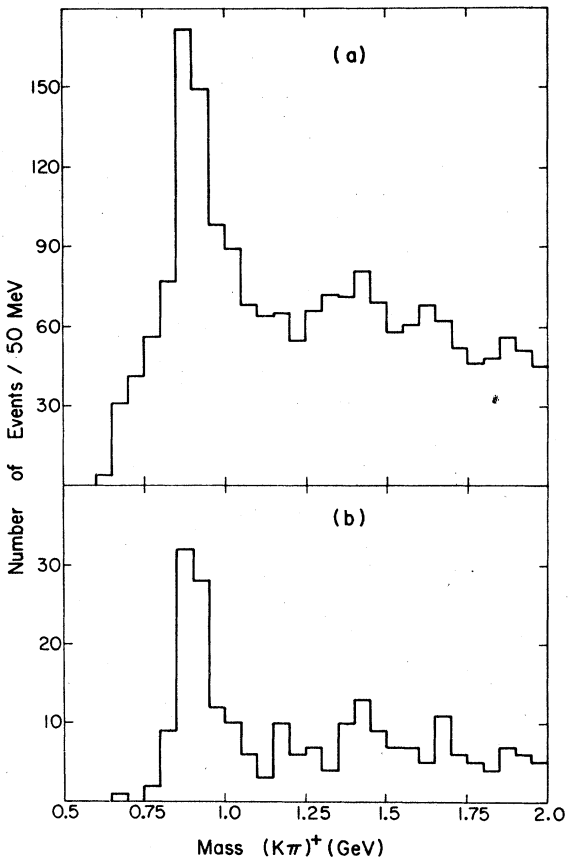

FIG. 11. $(K\pi)^+$ mass distribution from $\Lambda K^0\pi^+\pi^+$ and $\Lambda K^+\pi^+\pi^0$ final states. (a) No selection. (b) Selecting the $\Lambda\pi^+$ recoil mass to have $1.35 < \text{mass}(\Lambda\pi^+) < 1.42$ GeV.

We found statistically significant nonzero decay-angular moments which require $J \geq \frac{3}{2}$ for the $\Sigma^+(1700)$ in the $\Sigma^+(1700)K^*(890)$ channel.[36] However, the contribution of the large background (approximately 50%) to the moments in these $\Lambda K 2\pi$ final states, makes interpretation of these moments harder than it is in the $\Lambda K^+\pi^+$ final state, where a similar moments analysis requires only $J \geq \frac{1}{2}$ for the $\Sigma^+(1700)$ enhancement.

In Table III we list the $K^{*+}(890)$ density matrix elements. These moments allow the natural (δ^+) and unnatural (δ^-) spin-parity exchange contributions to $\Sigma^+(1700)K^{*+}(890)$ production[37] to be extracted:

$$\delta^+ = \rho_{11} + \rho_{1-1},$$

$$\delta^- = \rho_{00} + \rho_{11} - \rho_{1-1}.$$

Once again, the large background makes the results difficult to interpret, although natural spin-parity exchange seems to dominate.

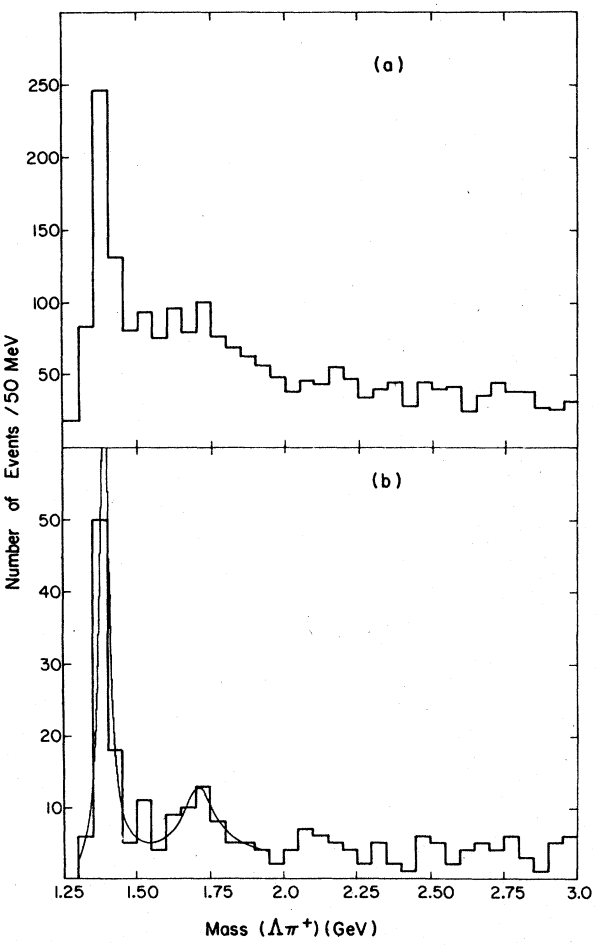

FIG. 12. $\Lambda\pi^+$ mass distribution from $\Lambda K^0\pi^+\pi^+$ and $\Lambda K^+\pi^+\pi^0$ final states. (a) No selection. (b) Selecting the $(K\pi)^+$ recoil mass to have $0.85 < \text{mass}(K\pi)^+ < 0.95$ GeV.

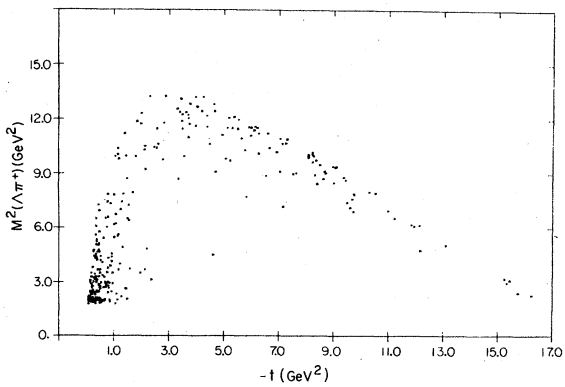

FIG. 13. Chew-Low plot for the events in Fig. 12(b).

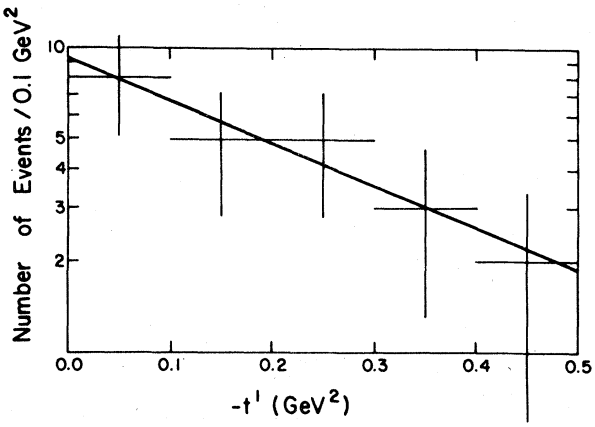

FIG. 14. $d\sigma/dt'$ for $\Sigma^+(1700)$ $K^{*+}(890)$ production. Curve shows the result of a fit to the form: $A\exp(bt')$.

We have also searched in the $\Lambda K3\pi$ and $\Lambda K4\pi$ final states for evidence of $\Sigma^+(1700)$ production. Figure 15 shows the $\Lambda\pi^+$ mass distribution from $\Lambda K3\pi$ and $\Lambda K4\pi$. There is no evidence for any bump in the $\Sigma^+(1700)$ region and selecting events with $-t(p \to Y^{*+}) < 1.0$ GeV^2 makes no difference.

We calculated the $\Sigma^+(1385)K^{*+}(890)$ cross section from the $\Lambda K2\pi$ final states using a slice technique.[38] The $(K\pi)^+$ mass distribution was sliced into bands and the amount of $\Sigma^+(1385)$ determined for each slice. This gave a determination of $\Sigma^+(1385)$ production as a function of $(K\pi)^+$ mass. Therefore, the amount of background and genuine quasi-two-body production could be obtained. The same procedure was followed using $\Lambda\pi^+$ mass slices and consistent results were obtained. We then assumed that the quasi-two-body events were distributed between the $\Lambda K^+\pi^+\pi^0$ and $\Lambda K^0\pi^+\pi^+$ final states according to the Clebsch-Gordan coupling for $K^{*+}(890)$ decay.[39] This gave a cross section of 3 ± 1 μb for

$$\pi^+p \to \Sigma^+(1385)K^{*+}(890).$$

Figure 16 shows this cross section as a function of laboratory momentum. Fitting the cross section to the form

TABLE III $K^{*+}(890)$ density matrix elements in the Gottfried-Jackson frame from the $\Sigma^+(1700)K^{*+}(890)$ final state ($-t' < 0.5$ GeV^2).

ρ_{00}	0.24 ± 0.14
ρ_{1-1}	0.33 ± 0.12
$\text{Re}\rho_{10}$	0.0 ± 0.08
δ^+	0.71 ± 0.16
δ^-	0.29 ± 0.16

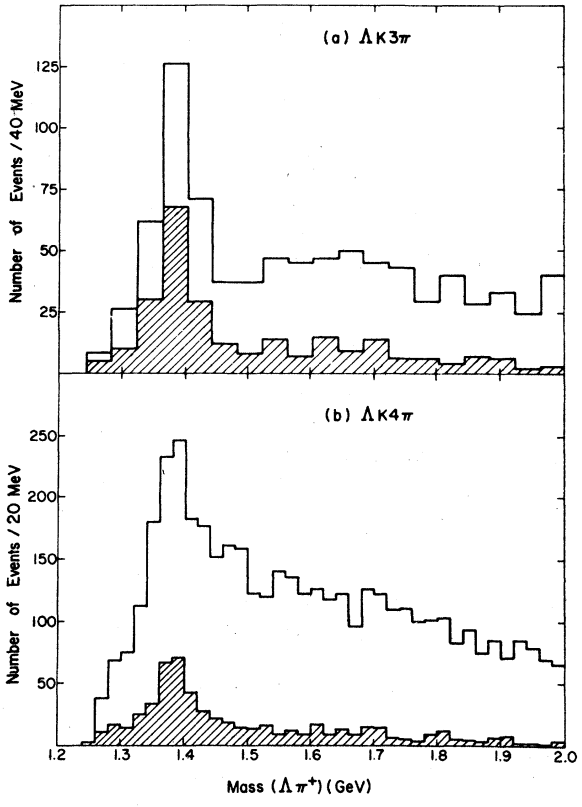

FIG. 15. $\Lambda\pi^+$ mass distributions from $\Lambda K 3\pi$ and $\Lambda K 4\pi$ final states. Shaded events show the effect of selecting $-t(p \to \Lambda\pi^+) < 1$ GeV^2.

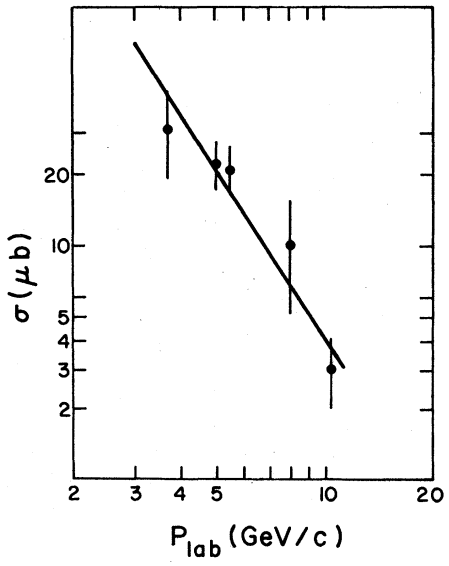

FIG. 16. $\Sigma^+(1385)$ $K^{*+}(890)$ production cross section as a function of laboratory momentum. The curve shows the result of a fit to $P_{\rm lab}{}^{-n}$, yielding $n = 2.4 \pm 0.4$.

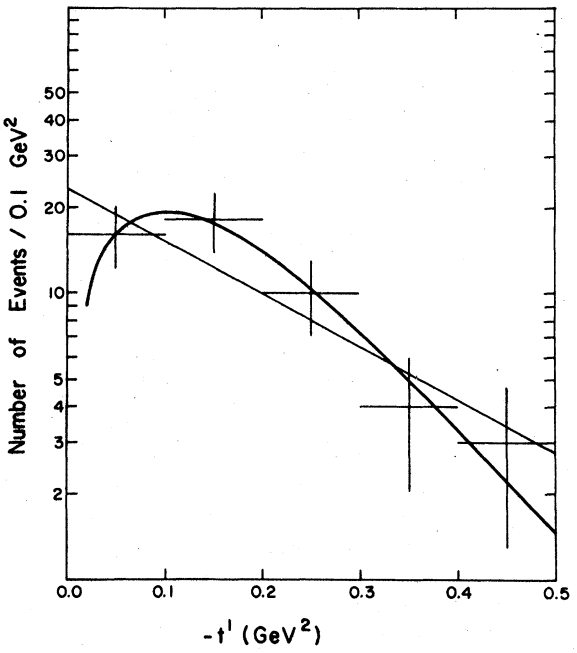

FIG. 17. $\Sigma^+(1385)$ $K^{*+}(890)$ differential cross section. Curves are fits to the forms: $A\exp(bt')$, $At'\exp(bt')$.

$$\sigma \propto P_{\rm lab}{}^{-n},$$

we obtain

$$n = 2.4 \pm 0.4.$$

Figure 17 shows the $\Sigma^+(1385)K^{*+}(890)$ differential cross section. There is some indication of a dip in the forward direction. The functions

$$t' e^{bt'}, e^{bt'}$$

both give acceptable fits, yielding $b = 10.5 \pm 1.0$, 4.2 ± 0.8 GeV^{-2}. Data at 3.7 GeV/c on this reaction[9] have also shown evidence for a turnover in the forward direction.

Table IV lists the $\Sigma^+(1385)$ and $K^{*+}(890)$ density matrix elements. They are similar to values obtained at lower energies[6-9] and the $\Sigma^+(1385)$ elements are roughly the same as in reaction (2) with the possible exception of $\mathrm{Re}\rho_{3-1}$. Again there appears to be both natural and unnatural spin-parity exchange. We estimate the background in this case to be about 25%.

The quark-additivity (class B) predictions for the density matrix elements are[34]

$$\rho_{11} = \tfrac{4}{3}\rho_{33},$$

$$\rho_{1-1} = \frac{4}{\sqrt{3}}\rho_{3-1},$$

$$\rho_{10} = \frac{4}{\sqrt{6}}\rho_{31}.$$

TABLE IV. Density matrix elements in the Gottfried-Jackson frame for the $\Sigma^+(1385)$ $K^{*+}(890)$ final state ($-t' < 0.5$ GeV^2).

$\Sigma^+(1385)$	
ρ_{33}	0.32 ± 0.07
$\mathrm{Re}\rho_{3-1}$	0.05 ± 0.07
$\mathrm{Re}\rho_{31}$	0.08 ± 0.07
$K^{*+}(890)$	
ρ_{00}	0.14 ± 0.08
ρ_{1-1}	0.20 ± 0.09
$\mathrm{Re}\rho_{10}$	0.0 ± 0.06
δ^+	0.63 ± 0.10
δ^-	0.37 ± 0.10

TABLE V. Test of quark-additivity predictions for $\Sigma^+(1385)K^{*+}(890)$ production.

Prediction	Data	
$\rho_{11} = \frac{4}{3}\rho_{33}$	0.43 ± 0.04	0.43 ± 0.09
$\rho_{1-1} = \frac{4}{\sqrt{3}}\rho_{3-1}$	0.33 ± 0.12	0.12 ± 0.16
$\rho_{10} = \frac{4}{\sqrt{6}}\rho_{31}$	0.00 ± 0.08	0.13 ± 0.11

As Table V indicates, these relations are satisfied within the rather large experimental errors. These class B equalities are obtained from the additivity postulate plus an additional assumption on the spin dependence of quark-quark scattering.[34] The class B predictions are generally found to give good agreement with a variety of different reactions.[35] Class C relations require further assumptions on the spin dependence of the quark-quark scattering amplitudes. These are, in general, found to disagree with experiment. In the present case the predictions are

$$\mathrm{Re}\rho_{31} = 0, \quad \mathrm{Re}\rho_{10} = 0,$$

and both of these do agree with our data.

CONCLUSIONS

We have examined

$\Sigma^+(1385)K^+$

and

$\Sigma^+(1385)K^{*+}(890)$

production in π^+p interactions at 10.3 GeV/c. We have shown that $\Sigma^+(1385)K^+$ production gives results which are consistent with a Regge-pole model[30,31] using vector and tensor K^* exchanged trajectories and incorporating dominant (Stodolsky-Sakurai) $M1$ coupling. This model reproduces the differential cross section for $-t' < 0.5$ GeV^2 and the spin density matrix elements in our data and gives a good representation of the production cross section as a function of beam momentum. The differential cross section for $\Sigma^+(1385)K^{*+}(890)$ production shows evidence for a turnover in the forward direction. The density matrix elements (averaged over t') agree with the class B and C quark-additivity predictions.

We have also observed an enhancement ($M = 1698 \pm 20$ MeV, $\Gamma = 240 \pm 60$ MeV) in the $\Lambda\pi^+$ mass distribution from the $\Lambda K^+\pi^+$ final state. This state also appears in the $\Lambda\pi^+$ mass distribution from the $\Lambda K^0\pi^+\pi^+$, $\Lambda K^+\pi^+\pi^0$ final states ($M = 1707 \pm 20$ MeV, $\Gamma = 130^{+100}_{-60}$ MeV) when we select events having a recoling $K^{*+}(890)$. The $\Sigma^+(1700)$ decay-angular moments in the $\Lambda K^+\pi^+$ final state are consistent with spin $\frac{1}{2}$. The moments in the $\Sigma^+(1700)K^{*+}(890)$ channel require $J \geq \frac{3}{2}$, but here the background is very large ($\sim 50\%$) requiring some caution in the interpretation of these moments.

ACKNOWLEDGMENTS

This experiment could not have taken place without the participation of a large number of people. We want to thank especially those physicists who took part in the early stages of the experiment and made important contributions to its progress: Dave Crennell, Dave Gilbert, Popat Patel, and Susan Vallet. Equally important was the work of measuring, scanning, programming, and data handling. In particular, we want to thank the following, who contributed so much in these areas: Quais Ashraf, Bruce Bolin, Rodney Jones, Peter Kahan, Dave Kesterton, June Liu, Sheila Maggs, Dave McDonald, John Phillips, Alfred Sipprell, and the large band of measurers and scanners at Toronto and Brookhaven. We also express our appreciation to the POLLY group and to all the members of the SLAC staff who contributed to the success of the data acquisition.

This research was supported in part by the National Research Council of Canada and by the U. S. Department of Energy under contract No. EY-76-C-02-0016.

[1]M. C. Goddard *et al.*, Phys. Rev. D 16, 7 (1977).
[2]M. C. Goddard *et al.*, Nucl. Phys. B 134, 49 (1978).
[3]Particle Data Group, Rev. Mod. Phys. 48, S1 (1976).
[4]D. H. Miller, in *Hyperon Resonances—70*, proceedings of a conference held at Duke University, 1970, edited by Earle C. Fowler (Moore, Durham, North Carolina, 1970), p. 229.
[5]Because of limited statistics we make no attempts to perform background subtractions for $d\sigma/dt'$ and the spin density matrix elements. Figures 1 and 2 show that the background under the $\Sigma(1385)$, and the $\Sigma(1700)$ in the $\Lambda K^+\pi^+$ final state is very small.
[6]M. Aderholz *et al.*, Nucl. Phys. B11, 259 (1969).
[7]W. Cooper *et al.*, Nucl. Phys. B23, 605 (1970).
[8]D. Toet *et al.*, Nucl. Phys. B63, 248 (1973).
[9]W. Butler *et al.*, Phys. Rev. D 7, 3177 (1973).
[10]A. Bashian *et al.*, Phys. Rev. D 4, 2677 (1971).
[11]P. Kalbaci *et al.*, Phys. Rev. Lett. 27, 74 (1971).
[12]S. Ying *et al.*, Phys. Lett. 30B, 289 (1969).
[13]D. Davies *et al.*, Phys. Rev. D 2, 506 (1970).
[14]Y. Pan and F. Forman, Nucl. Phys. B21, 395 (1970).
[15]A. Berglund *et al.*, Phys. Lett. 60B, 117 (1975).
[16]P. Hanson *et al.*, Phys. Rev. D 4, 1296 (1971).
[17]M. Aderholz *et al.*, Nucl. Phys. B7, 111 (1968).
[18]B. Chourand *et al.*, Nucl. Phys. B117, 1 (1976).
[19]S. Holmgren *et al.*, Nucl. Phys. B119, 261 (1977).
[20]M. Goddard, Ph.D. thesis, University of Toronto, 1977 (unpublished).
[21]G. Girardi and H. Navelet, Nucl. Phys. B116, 168 (1976).
[22]L. Stodolsky and J. Sakurai, Phys. Rev. Lett. 11, 90 (1963).
[23]L. Stodolsky, Phys. Rev. 134, B1099 (1964).
[24]N. Schmitz and H. Pilkuhn, in Proceedings of the CERN 1965 Easter School, Vol. 1, CERN Report No. 65-24 (unpublished).
[25]These two reference systems are equivalent in the Stodolsky-Sakurai model. A decay-angular distribution of the form $(1+3\cos^2\theta)$ is invariant under any rotation around the production normal. Just such a rotation connects (at fixed t) the helicity and Gottfried-Jackson frames.
[26]We quote our results in terms of t'; however, in making comparisons with theoretical models we neglect the small difference between t and t' ($t_{\min} \simeq -0.01$ GeV^2).
[27]J. Mott, Nucl. Phys. B13, 565 (1969).
[28]D. Griffiths and R. Jabbur, Nucl. Phys. B11, 7 (1969).
[29]F. Eysel *et al.*, Z. Phys. 199, 411 (1967).
[30]G. Renninger and K. Sarma, Phys. Rev. 178, 2201 (1969).
[31]G. Renninger and K. Sarma, Phys. Rev. D 2, 1281 (1970).
[32]A. Bialas, A. Kotanski, and K. Zalewski, Nucl. Phys. B28, 1 (1971).
[33]H. Lipkin, Nucl. Phys. B1, 597 (1967).
[34]A. Bialas and K. Zalewski, Nucl. Phys. B6, 465 (1968).
[35]F. Schrempp and B. Schrempp, in *High Energy Physics*, proceedings of the European Physical Society International Conference, Palermo, 1975, edited by A. Zichichi (Editrice Compositori, Bologna, 1976), p. 682.
[36]The hypothesis that $t_{LM}=0$; $L=2,3$ leads to a χ^2/df of 14/6.
[37]J. Ader *et al.*, Nuovo Cimento 56A, 952 (1968).
[38]M. Aguilar-Benitez *et al.*, Phys. Rev. D 5, 11 (1972).
[39]This is necessary because we do not have sufficient statistics to perform the slice technique on the $\Lambda K^+\pi^+\pi^0$ and $\Lambda K^0\pi^+\pi^+$ final state separately. This assumption is consistent with selecting $\Sigma^+(1385)$ $K^*_+(890)$ events from the $\Lambda K^0\pi^+\pi^+$, $\Lambda K^+\pi^+\pi^0$ final states separately using broader bands than is necessary for the slice technique.